High-pressure amorphous phase of vanadium pentaoxide

A. K. Arora,[1,*] Tomoko Sato,[2] Taku Okada,[2] and Takehiko Yagi[2]
[1]*Materials Science Division, Indira Gandhi Centre for Atomic Research, Kalpakkam 603102, India*
[2]*Institute for Solid State Physics, The University of Tokyo, Kashiwa, Chiba 277-8581, Japan*
(Received 28 October 2011; revised manuscript received 26 January 2012; published 30 March 2012)

We have discovered a high-pressure amorphous state of vanadium pentaoxide based on the results of an *in situ* high-pressure Raman spectroscopic and synchrotron x-ray diffraction study in a diamond-anvil cell up to 53 GPa under nonhydrostatic conditions. The broadening of Raman spectra and the diminishing of diffraction intensities suggest the evolution of disorder in the high-pressure β phase. The compound has been found to undergo amorphization around 40 GPa. Upon the release of pressure, the material remains amorphous; however, the changes in the shapes of the structure factor and pair correlation function suggest that a-V_2O_5 recovered after pressure cycling is different from that at high pressure, indicating possible polyamorphism. Raman investigations show that unlike α and β crystalline phases, the high-pressure amorphous phase contains only doubly coordinated oxygen. A comparison of the Raman spectrum of a-V_2O_5 recovered from high pressure with that of the vapor-deposited a-V_2O_5 film suggests that although both of these have disordered arrangements of V=O bonds, their structures are not identical.

DOI: 10.1103/PhysRevB.85.094113 PACS number(s): 61.43.Er, 64.70.K−, 78.30.−j

I. INTRODUCTION

It has been a challenge to obtain a crystalline compound in a metastable amorphous/glassy state.[1] By following the rapid solidification route, it is relatively simple to obtain a vitreous state in a binary[2] or ternary[3] system, in which one of the components is a glass former. Although such systems can have numerous applications,[4] obtaining an understanding of the structure in a multicomponent glass is nontrivial. Among the elements and compounds, the systems with strong covalent bonds, such as Si, S, Se, Te, SiO_2, B_2O_3, and several others, are easily obtainable either as a glass or as an amorphous solid. From the point of view of amorphization, it is important to point out that other than rapid solidification, the application of high pressure is often helpful in creating an amorphous state[5] if a structural transition from one crystalline state to another is kinetically hindered.[6] Pressure-induced amorphization has been reported in a large number of systems.[7] The structure of pressure-amorphized quartz[8] is found to be different from that of melt-quenched SiO_2 glass.[9] Similarly, high-density amorphous forms have also been reported in ice[10] and amorphous-Si.[11] In view of this, it is of fundamental interest to examine other glass-forming compounds if these also become amorphous at high pressure. We have chosen V_2O_5 for the high-pressure study because its glassy/amorphous state, formed by splat-cooling[12] (bulk) and physical vapor deposition[13] (thin film), is well established. The aim of the present study is to explore the possibility of obtaining V_2O_5 in an amorphous form at high pressure.

In recent years, vanadium pentaoxide has attracted considerable attention due to interesting semiconducting properties and applications in catalysis, solar-cell windows, gas- and moisture-sensing, optoelectronic switching devices, and lithium-ion batteries.[14–17] Amorphous V_2O_5 films have also been investigated extensively.[18–22] Several high-pressure and high-temperature studies have been carried out on V_2O_5, and two structural phase transitions to high-pressure polymorphs have been reported.[23–29] The ambient pressure α phase has a layered orthorhombic structure with corner- and edge-sharing VO_5 square pyramids. Above 7 GPa, the high-pressure monoclinic (β) phase consists of chains of quadruple units of edge-sharing VO_6 octahedra along the b axis.[28] Figure 1 shows structures of α and β phases. A VO_6 octahedron in the β phase is formed when apex oxygen of the VO_5 square pyramid forms a bond with the V atom of the pyramid of the adjacent layer. A transition to another monoclinic phase (δ) has also been identified above 15 GPa.[29] Based on the studies carried out on different polymorphs of V_2O_5 recovered after high-pressure high-temperature treatment in large-volume presses, two high-pressure polymorphs β and δ were identified with monoclinic structures. The ambient pressure α phase has a volume of 89.6 Å^3 per formula unit, while those of β and δ phases are 80.06 and 72.58 Å^3, respectively. This compound has not been investigated above 29 GPa. Diamond-anvil-cell-based Raman and x-ray diffraction measurements have revealed only the α-β transition occurring around 6–7 GPa.[24,27] In the present work, we have carried out *in situ* high-pressure x-ray diffraction on V_2O_5 up to 53 GPa in a diamond-anvil cell (DAC) using synchrotron radiation and high-pressure Raman spectroscopy also up to 53 GPa to explore the possibility of obtaining an amorphous state at high pressure. The sample is indeed found to become amorphous at 41 GPa. The diffraction patterns were analyzed quantitatively to obtain the structure factor and the pair correlation function. The diffraction and the Raman spectrum from the amorphous state in the samples recovered from the highest pressure are also measured and compared with that reported for amorphous V_2O_5 films synthesized using physical vapor deposition.

II. EXPERIMENTAL DETAILS

Powdered samples of polycrystalline V_2O_5 (purity 99.9%) were loaded into a 160-μm hole of a stainless-steel gasket (preindented to 70-μm thickness) of a Mao-Bell-type high-pressure DAC. In the DAC, no pressure-transmitting medium was used. The reason for not using a pressure-transmitting medium will be discussed in the next section. *In situ* x-ray diffraction measurements were performed using synchrotron

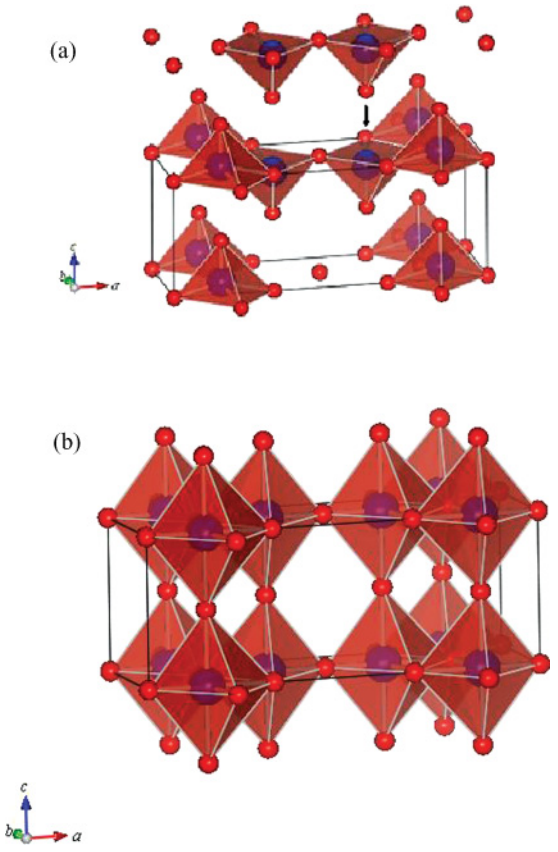

FIG. 1. (Color online) Structures of the ambient pressure orthorhombic α phase (a) and the high-pressure monoclinic β phase (b) of V_2O_5. Due to compression along the c axis, the terminal oxygen from the neighboring layer (marked by an arrow) moves closer to the base of the VO_5 square pyramid and pulls the vanadium atom closer, thereby stretching the V=O bond. The terminal oxygen eventually forms the vertex of the VO_6 octahedron in the β phase.

radiation [$\lambda = 0.4131(2)$ Å] from the NE1 beamline at AR-Photon Factory, KEK. A 30-μm collimator was used and an y-z translation stage was used to align the sample in the hole of the gasket with the collimator. A thin gold foil of 30-μm size was also placed within the gasket hole, and the pressure was obtained from the equation of state of gold.[30] The DAC was translated to bring either the sample area free from gold foil or that containing it in front of the collimator. An image plate of size 30 cm $\times$ 30 cm (Rigaku R-axis-7) with a readout resolution of 100 μm was used as the detector. Synchrotron measurements were performed at successively higher pressures up to 53 GPa. After reaching the highest pressure, the pressure was reduced gradually and the diffraction pattern was also measured (in the DAC) after releasing the pressure. Due to limited beam time, no diffraction measurements were done in the pressure-reducing cycle. Immediately after completing the synchrotron measurements, the DAC background was measured separately using the same (empty) DAC without any sample. The lack of a pressure-transmitting medium can cause some pressure gradients to occur within the hole of the gasket. It must be emphasized that the DAC could be positioned reproducibly within 1 μm, and the measurements were performed at the same spot each time and the beam diameter was much less than the gasket hole. Thus the diffraction originated from the same region of the material, as measurements were done at successively higher pressures. The spread in pressure within the 30-μm beam area (due to the pressure gradient) was estimated to be less than 1 GPa. Raman spectra in the DAC were excited using 100-mW power at the 514.5-nm line from an argon-ion laser. The spectra were recorded using a micro-Raman setup described elsewhere.[7] With a 20 $\times$ long working-distance objective, the spot size was about 3 μm. Raman measurements were also performed during the pressure-reducing cycle. The spectrum of recovered samples outside the DAC was recorded using 5-mW power. For Raman experiments, pressure was measured using the ruby fluorescence method.

III. RESULTS AND DISCUSSION

A. High-pressure x-ray diffraction

The effects of nonhydrostatic pressure or nonhydrostaticity in the DAC on the high-pressure behavior of materials have been investigated on a variety of compounds and systems.[31–35] The observed effects are (a) changes in the sequence of phase transitions, (b) the appearance of metastable phases, (c) the growth of positional disorder, and (d) amorphization. The presence of deviatoric and shear stresses due to nonhydrostaticity is expected to cause a severe distortion of the lattice. The growth of disorder beyond a critical value may eventually lead to the loss of long-range order. As the aim of the present study is to see if V_2O_5 can become amorphous at high pressure, no pressure-transmitting medium was used. The absolute diffraction intensity depends on the synchrotron ring current and the exposure time of the image plate. In view of this, the diffraction intensities were normalized to a constant ring current and a constant exposure time. Figure 2 shows the normalized diffraction patterns of V_2O_5 up to a pressure of 37 GPa. One can see that in addition to the appearance of new peaks, the intensities of the diffraction peaks diminish gradually and also become broad. The intensities of peaks characteristic of the α phase decrease, while those of the peaks corresponding to the β phase increase. This arises due to two-phase coexistence over a range of pressures. The α-β transition is well documented,[24] and severe anisotropic peak broadening accompanying the transition has also been reported earlier. In the pattern at 37.4 GPa, hardly any diffraction peak is discernable. The cell parameters estimated from the data are found to be in agreement with those reported.[24] It should be pointed out that earlier high-pressure studies on V_2O_5 using nitrogen (a nearly hydrostatic medium) and paraffin oil have shown identical results.[24]

The reduction in the diffraction intensities and broadening suggests the evolution of disorder at high pressure. The anisotropic broadening reported earlier has been attributed to pronounced structural disorder in the high-pressure phase.[24] Among other diffraction peaks, one can notice an unambiguous and systematic decrease of the (200) diffraction peak intensity. This suggests that the disorder evolves in the bc plane containing edge-sharing square pyramids as the interplanar coupling is via corner-shared oxygen atoms. At 30 GPa, most of the diffraction peaks disappear, and at 37.4 GPa these also

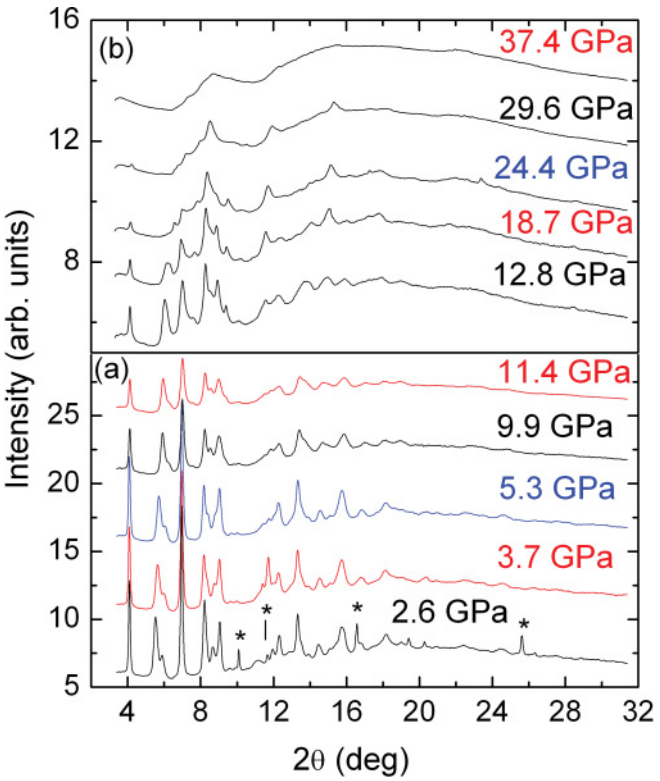

FIG. 2. (Color online) Diffraction patterns of V_2O_5 at high pressures. The peaks labeled with an asterisk in the 2.6 GPa pattern correspond to gold. The region containing gold was carefully avoided while recording diffraction from the sample at higher pressures.

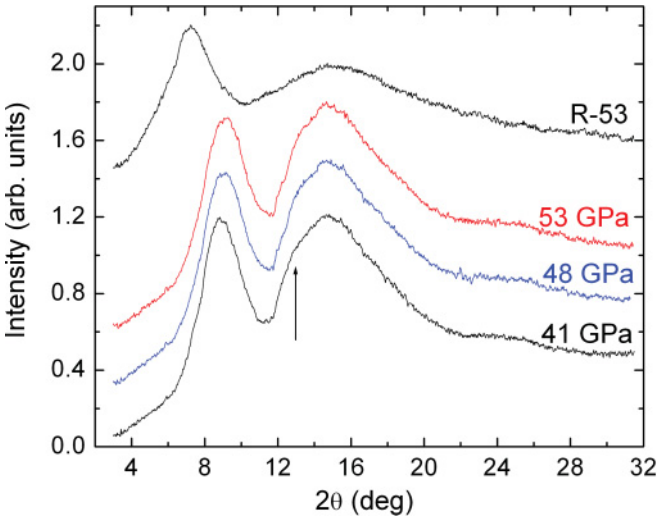

FIG. 3. (Color online) The diffraction patterns of pressure-amorphized V_2O_5 after correcting for the DAC background. The pattern labeled R-53 is that of the recovered sample at ambient pressure after subjecting it to 53 GPa. The vertical arrow shows the position of the shoulder.

vanish leaving only a broad intensity profile with a kink at the position of the most prominent diffraction at 8.8° 2θ. This suggests that the sample is on the verge of turning amorphous. The diffraction patterns above 40 GPa are shown in Fig. 3 after subtracting the DAC background. The DAC background was subtracted using the procedure described in Ref. 38. These patterns correspond unambiguously to an amorphous state with broad peaks centered at 8.8 and 14.6° 2θ. The first peak shifts to higher 2θ as pressure is increased further due to the compression of the amorphous state. Figure 3 also shows the diffraction pattern measured after releasing the pressure from 53 GPa. The persistence of the broad peaks in the recovered pattern suggests that the recovered sample remains in the amorphous state. Thus the present results show that V_2O_5 undergoes irreversible amorphization at high pressure similar to that found in many network structures.[6,7,36]

In order to obtain further insight into the structure of the high-pressure amorphous state, the diffraction patterns were quantitatively analyzed to obtain the structure factor $S(Q)$. For this, the background-subtracted patterns were corrected for (a) θ-dependent attenuation in the sample, (b) incoherent scattering, and (c) atomic form factors using a procedure outlined earlier.[37] Figure 4(a) shows the structure factors of amorphous-V_2O_5 at high pressure. Three clear broad peaks are found in the patterns where the second peak exhibits a shoulder around 3.4 $Å^{-1}$. Such a shoulder on the low-Q side of the second peak is not commonly found in most glasses/amorphous solids and appears to be unique to high-pressure a-V_2O_5. Furthermore, the height of the second peak is also greater than that of the first. This is again uncommon. Further insight about what structure (at a microscopic level) causes these uncommon features can emerge from reverse Monte-Carlo fitting of the $S(Q)$. The structure factor of the sample recovered from 53 GPa, shown in Fig. 4(b), is significantly different from those of Fig. 4(a) in terms of the shapes of the peaks. The recovered a-V_2O_5 does not exhibit the shoulder found at high pressure. Furthermore, similar to most amorphous solids, the height of the second peak is smaller than that of the first. These differences suggest considerable structural modifications upon the release of pressure. One can see that the differences between the $S(Q)$'s at 53 GPa and that of the R-53 sample are dramatic and cannot occur from a monotonic shift of diffraction as a function of pressure within a single phase. In view of this, the structure of the recovered a-V_2O_5 appears to be different from that of a-V_2O_5 at high pressure. Thus the present results are suggestive of polyamorphism. At high pressure, the scattering vector Q_1 corresponding to the position of the first peak shifts to larger Q, suggesting further compression at high pressure. Upon releasing the pressure, the first peak position exhibits a large downshift and the second peak becomes broader. The values of Q_1 in the amorphous state, shown in the inset of Fig. 4(b) as a function of pressure, are found to exhibit a monotonic increase with pressure. Note that the data corresponding to the recovered sample do not lie on the linear fit extrapolated to $P = 0$. We now discuss possible reasons for this. As the P dependence of Q_1 is governed by the compressibility, this is expected to be nonlinear in the low-pressure region, as in the case of a standard equation of state. The expected nonlinear behavior is schematically shown in the inset as a dashed curve. However, this would imply that the high-pressure a-V_2O_5 phase is recoverable to the ambient. On the other hand, the qualitative differences in the shapes of the peaks of $S(Q)$ suggest the opposite. Detailed extended x-ray-absorption fine-structure (EXAFS) investigations would be able to further

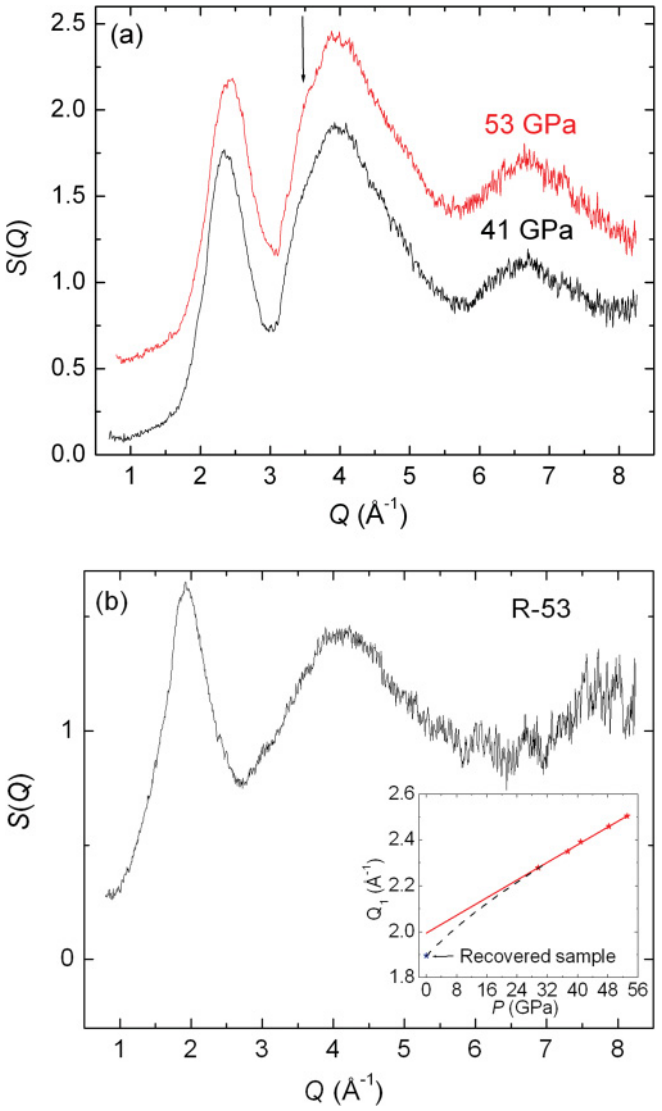

FIG. 4. (Color online) (a) Structure factor of a-V_2O_5 at different pressures. The vertical arrow shows the position of the shoulder. (b) $S(Q)$ of the amorphous sample recovered from 53 GPa. The inset shows the position of the first diffraction peak of the amorphous sample. The data labeled "recovered sample" correspond to the sample recovered from 53 GPa. Straight line is the linear fit to the high-pressure data. Dashed curve is a guide to the eye.

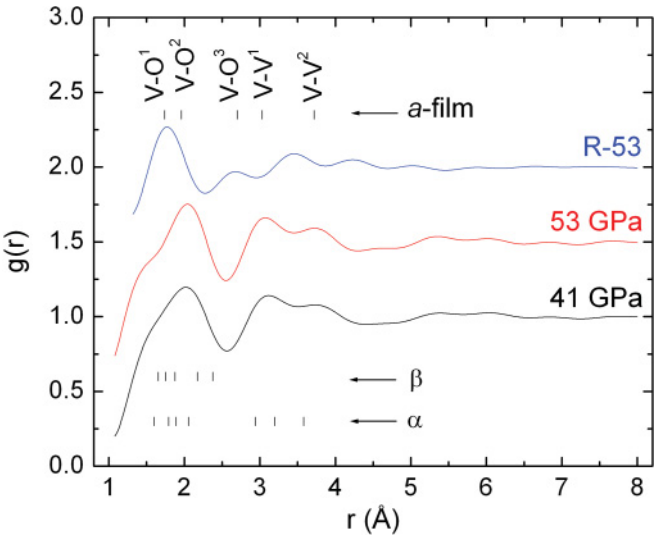

FIG. 5. (Color online) Pair correlation functions $g(r)$ obtained by Fourier transforming $S(Q)$ of V_2O_5 at 41 and 53 GPa and that of the sample recovered from 53 GPa (R-53). The reported V-O and V-V atomic distances in crystalline α and β phases (Refs. 25 and 40) and those in an amorphous film (Ref. 18) are shown as tick marks. Distances larger than 3 Å correspond to V-V distances.

elucidate the differences in the local structure of the two amorphous states.

In order to obtain insight into the real-space structure of the pressure-amorphized V_2O_5, the pair correlation function $g(r)$ was obtained by Fourier transforming $S(Q)$ with MATLAB using a procedure described earlier.[37] As the $S(q)$ data are available only up to a certain q, the range of integration becomes finite. This is known to result in spurious high-frequency oscillations in the calculated $g(r)$. To avoid such spurious oscillations, Blackman[38] or sinc[39] windows are often employed for integration. In the present analysis, $g(r)$ was calculated using a sinc window. Figure 5 shows the $g(r)$'s at different pressures, including that of the amorphous sample recovered from 53 GPa. The first peak in $g(r)$ at 41 GPa is broad and exhibits a shoulder at $r \sim 1.5$ Å, which shifts to the left when pressure is increased to 53 GPa. A comparison of the reported V–O bond distances in the crystalline phases[25] and an amorphous film[18] with those in the high-pressure amorphous state suggests that the first peak consists of mainly the V-O distances. Broadening of the first peak due to the shift of the shoulder to lower r at 53 GPa implies that in the high-pressure a-V_2O_5 form, the V–O bonds have a wider spread. The second and the third peaks occur at $\sim$ 3.1 and 3.7 Å and essentially correspond to V-V distances.[40] Thus one can visualize the structure of a-V_2O_5 as a random arrangement of the severely distorted VO_n polyhedra where the distribution of the V–O bond distance increases further at higher pressures.

A comparison of the $g(r)$ of the recovered amorphous sample upon the release of pressure with that at 53 GPa reveals that the shoulder of the first peak is absent. Furthermore, from the widely different shapes of the $g(r)$'s of the recovered sample and that at 53 GPa, the two amorphous forms appear to be different. Had the two amorphous forms been structurally the same, the features in the $g(r)$ curves would have shown only a systematic shift. This argument is in agreement with the inference drawn from the differences in the features in the $S(Q)$'s of the recovered amorphous sample and that at 53 GPa. It is worth comparing the reported V-O and V-V atomic distances in an amorphous film with the features in the $g(r)$ of the recovered amorphous form. One can see from Fig. 5 that the V-O distances found in the amorphous film lie within the peaks of $g(r)$; however, the V-V atomic distances do not correspond to the peaks in $g(r)$ of the recovered sample. This suggests that the medium-range order in the amorphous film could be different from those in the recovered amorphous sample. Differences and similarities between different possible amorphous forms will be discussed again after presenting the results of the Raman investigations.

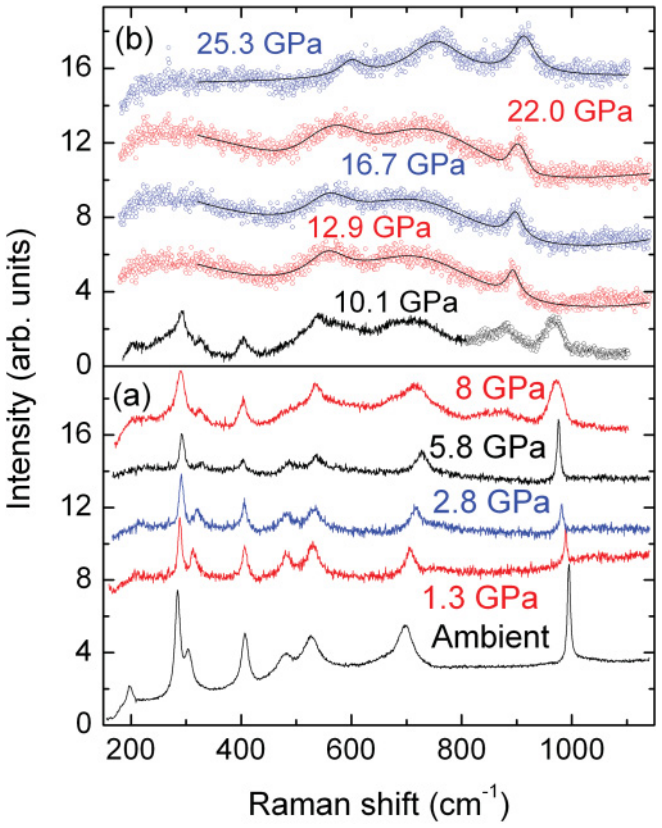

FIG. 6. (Color online) Raman spectra of V_2O_5 at different pressures, (a) in the orthorhombic phase and (b) in the high-pressure monoclinic phase. Between 8 and 10 GPa, the two phases are found to coexist. Solid curves are the Lorentzian least-square fits to the data including a suitable background.

B. High-pressure Raman spectroscopy

In order to examine the changes that occur in the phonon spectrum of V_2O_5 at high pressure, we have measured *in situ* Raman spectra in the DAC up to 53 GPa. Figure 6 shows the Raman spectra between ambient and 25.3 GPa. Several prominent peaks characteristic of the α phase are seen in the ambient pressure spectrum. The sharp peak at 995 cm^{-1} has been attributed to the stretching vibration of the terminal oxygen (V=O bond) in the VO_5 square pyramid.[41] The mode at 706 cm^{-1} is attributed to the doubly coordinated oxygen stretching vibration resulting from corner-shared oxygen common to two pyramids (V_2-O), whereas that at 530 cm^{-1} is attributed to the triply coordinated oxygen stretching mode arising from edge-shared oxygen common to three pyramids (V_3-O).[42,43] The peaks at 405 and 283 cm^{-1} are attributed to the bending vibrations of the V=O bond, whereas those at 487 and 303 cm^{-1} are attributed to the bending vibrations of the bridging V_2-O and V_3-O bonds, respe ctively.[42,44] The low-frequency modes correspond to the lattice modes.

At high pressure, one can see that the V=O stretching vibration mode shifts to lower wave numbers. Under the influence of pressure, the vibrational mode frequencies are normally expected to increase as bonds are compressed. On the other hand, a few modes are sometimes found to show the opposite behavior. The existence of such soft modes suggests instability of the system against a possible structural phase transition. The decrease of the 995-cm^{-1} mode frequency in the present case thus suggests elongation of the V=O bond at high pressure. Here we present a physical model for the evolution of the system at high pressure. This can happen because of the compression of the *c* axis (the *a* parameter increases slightly while the *b* parameter decreases marginally at high pressure). The oxygen of the neighboring layer moves toward the base of the square pyramid and pulls the V atom closer to the base [shown by the arrow in Fig. 1(a)], making the V=O bond weaker and elongated. The peaks of most other modes shift to higher wave numbers as expected for normal behavior. The 995-cm^{-1} soft mode eventually drives the transition to the monoclinic structure where VO_5 square pyramids transform to VO_6 distorted octahedra with the help of oxygen of the neighboring layer. This transition causes a large discontinuous decrease in the V=O stretching frequency to 883 cm^{-1} due to further elongation of the V=O bond. Decrease in the V=O stretching frequency has earlier been interpreted as a V^{5+} to V^{4+} valence transition based on the mode behavior in V_2O_5-MoO_3 solid solution.[27] The alternate perspective presented here for understanding the changes in the Raman mode frequency is consistent with the reported longer V=O bond (1.654 Å) in the β phase compared to that (1.601 Å) in α phase at ambient.[25]

Between 8 and 10 GPa, modes of both α and β phases are found in the spectra, suggesting a coexistence of the phases over this pressure range. In the high-pressure β phase the Raman peaks are very weak, possibly because of the existence of disorder, which is consistent with the findings of the present x-ray diffraction measurements. A much weaker Raman spectrum of the β phase has been found earlier also,[27] where measurements were performed only up to 12 GPa. As the signal was weak in the high-pressure phase, the spectra were fitted to Lorentzian line shapes with a suitable background using PEAKFIT, and peak centers were obtained. The typical standard errors were 2, 3, and 1 cm^{-1} for the 540-, 762-, and 886-cm^{-1} modes, respectively. In the high-pressure phase, the V=O stretching mode shifts to higher wave numbers exhibiting normal behavior, suggesting a uniform compression of the VO_6 octahedra. Only three modes centered at 540, 762, and 886 cm^{-1} could be followed up to a pressure of 25 GPa. These modes essentially arise from the vibrations of triply, doubly, and singly coordinated oxygen atoms, respectively. It is important to point out that in complete contrast to the present *in situ* spectra, Balog *et al.*[29] have reported the Raman spectra for β and δ phases (recovered from HP-HT treatment) at ambient being nearly identical to that of the α phase. This may be due to the transformation of the β and δ phases back to the α phase due to laser heating of the sample. The effect of laser heating on the Raman spectra will be discussed later in more detail. The pressure dependence of the mode frequencies is shown in Fig. 7. In the high-pressure β phase, the modes at 886 and 540 cm^{-1} exhibit hardening while that at 762 cm^{-1} shows the opposite behavior. Table I gives the pressure coefficients and Gruneisen parameters of the phonon modes in the two phases. The Gruneisen parameters for the α phase are calculated using the reported value of the bulk modulus.[24]

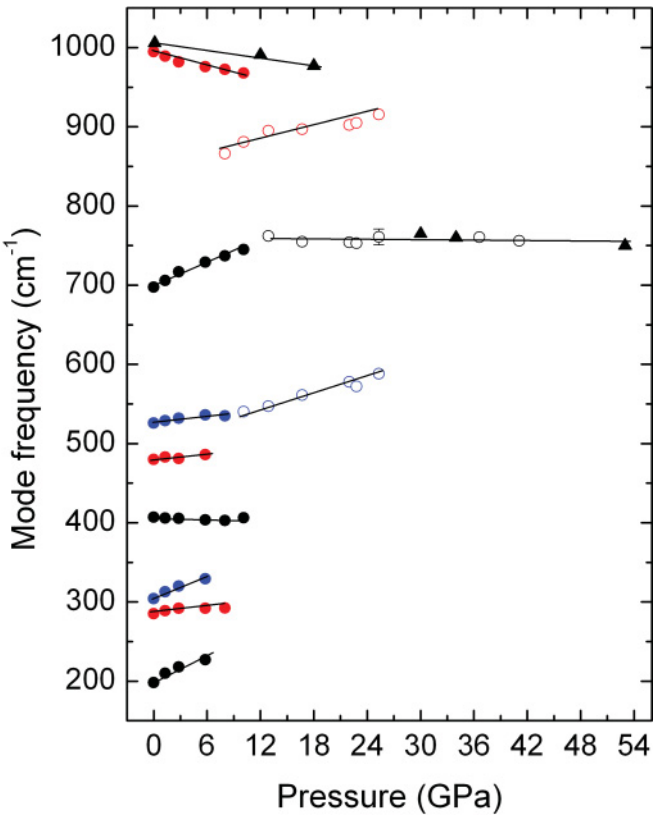

FIG. 7. (Color online) Mode frequencies as a function of pressure. A few modes are found to be soft in the ambient pressure orthorhombic phase as well as in the high-pressure phase. Open symbols are the modes in the β phase and above 36 GPa in the amorphous state. Filled triangles correspond to the data from the P-reducing cycle.

It should be pointed out that Raman spectroscopy is a powerful technique for the identification of different types of polyhedral units in the disordered systems from the existence of the characteristic vibrational frequencies of different types of structural units. Figure 8(a) shows the Raman spectra in the high-pressure amorphous state. Here only one broad peak is observed at 755 cm^{-1}, which actually continues from the

TABLE I. Pressure coefficients and Gruneisen parameters of Raman modes in the ambient and high-pressure phases of V_2O_5. The numbers in parentheses are standard errors in the least significant digits.

Mode (cm^{-1})	P coefficient (cm^{-1} GPa^{-1})	Gruneisen parameter
198	4.8(9)	1.2(2)
285	1.1(5)	0.19(8)
304	4.1(6)	0.67(10)
407	− 0.59(4)	− 0.072(5)
480	0.9(4)	0.09(4)
526	1.7(2)	0.16(2)
540 (β)	2.8(6)	
697	5.4(6)	0.39(4)
762 (β)	− 0.80(26)	
886 (β)	0.95(17)	
993	− 3.2(5)	− 0.16(2)

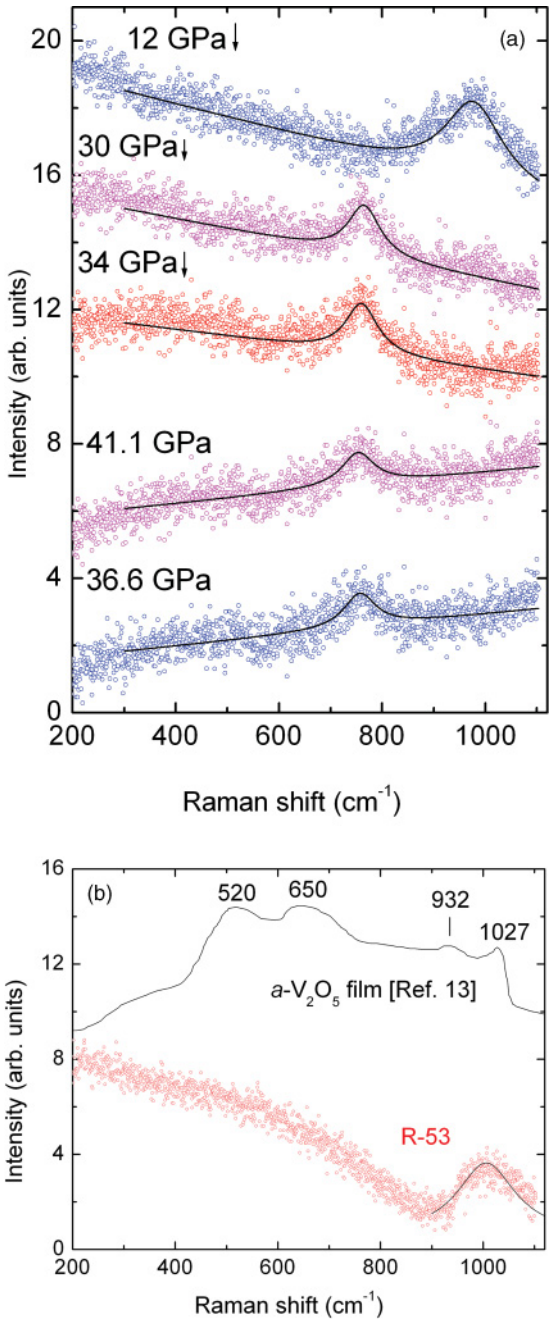

FIG. 8. (Color online) (a) Raman spectra of high-pressure amorphous forms of V_2O_5. Spectra labeled with a down-arrow correspond to the P-reducing cycle. Solid curves are the Lorentzian least-squares fits to the data including a suitable background. (b) Raman spectrum of a-V_2O_5 after recovering at ambient. For comparison, the Raman spectrum of vapor-deposited V_2O_5 reported by Lee *et al.* (Ref. 13) is also included.

β phase. This represents the average V-O stretching vibration frequency corresponding to the average V-O bond distance in the amorphous state. The mode frequency, when extrapolated to the ambient, is around 757 cm^{-1}, which is close to the doubly coordinated (V-O-V) vibrations of the oxygen. This suggests that the high-pressure a-V_2O_5 form has predominantly V_2-O-type bonds. If one compares the Raman spectrum at 25.3 GPa [Fig. 6(b)] with that at 36.6 GPa [Fig. 8(a)], one can see that

prior to amorphization, only the doubly coordinated (V_2-O) oxygen vibrations survive while singly and triply coordinated oxygen modes disappear. From the Raman spectra measured during the pressure-reducing cycle, one can see that at 12 GPa, the 755-cm^{-1} mode disappears and a new mode around 1000 cm^{-1} appears. This confirms the occurrence of an amorphous-amorphous transition, inferred from diffraction results, upon the release of pressure. The mode frequencies during the pressure-reducing cycle are also included in Fig. 7.

Upon releasing the pressure, the recovered a-V_2O_5 continues to exhibit a broad Raman peak near 1000 cm^{-1} [Fig. 8(b)] close to the mode frequency for V=O stretching vibration at ambient (995 cm^{-1}). This implies the restoration or reformation of V=O-like bonds in the recovered amorphous state. Thus the recovered a-V_2O_5 appears to have a random arrangement of VO_5-like structural units similar to those of α-V_2O_5. The reason for the high background toward low wave numbers is not well understood. This may occur due to the continuum arising from the vibrational density of states. The present Raman scattering results suggest that the nature of bonds and hence the structure of the recovered a-V_2O_5 is different from that at high pressure, and the high-pressure amorphous form is not quenchable to the ambient. This conclusion is in agreement with the inference drawn from the behaviors of $S(Q)$ and $g(r)$. Thus the present results indicate the possibility of polyamorphism in this system. It should be pointed out that when a laser power of 100 mW was used on the recovered sample kept outside the DAC, a recrystallization of the sample was found to occur. Hence recovered samples were investigated using only 5 mW. On the other hand, use of 100-mW power on the sample in the DAC at high pressure did not cause any recrystallization, possibly because of the sample being in contact with the diamond culet, which is an excellent thermal conductor. Splat-cooled glassy V_2O_5 is known to recrystallize at relatively low temperature of 185 °C.[26]

A comparison of the vibrational spectra of the recovered and vapor-deposited a-V_2O_5 forms is in order. For this, the reported[13] Raman spectrum of vapor-deposited a-V_2O_5 film is also included in Fig. 8(b). One can see the presence of prominent peaks at 520, 650, 932, and 1027 cm^{-1}. The peaks at 520, 650, and 1027 cm^{-1} have been attributed to vibrations of triply, doubly, and singly coordinated oxygen atoms, respectively, in analogy with those of the α phase. The 932-cm^{-1} mode in the amorphous film has been attributed to the $V^{4+} = O$ unit and the film is argued to have vanadium in a $+5$ and $+4$ mixed valence state. A change in the oxidation state of vanadium can arise due to a small departure of oxygen stoichiometry in the film or due to doping with a monovalent impurity ion.[13] In the film, the V=O vibrational frequency occurs at 1027 cm^{-1}. The difference in the vibrational frequencies of the V=O mode in the film and the recovered amorphous form could be due to the differences in the intermediate-range order, as the vibrational frequency of any given bond is strongly influenced by its immediate neighborhood. From the existence of the V=O bonds in both cases, one can say that the two structures are similar but not identical. The amorphous/glassy materials obtained by vapor deposition/rapid solidification are known to have lower bulk densities than their crystalline counterparts because of the existence of open volume defects that have a size distribution.[45] Low- and high-density amorphous forms[46,47] have been reported from the large volume experiments only in a limited number of simple systems, such as quartz,[8,9] GeO_2,[48] ice,[10] and Si,[11,38] and more recently in zirconium tungstate,[49] which has a complex network structure. However, in view of the extremely small quantity of the sample recovered from the DAC and also in the amorphous thin film, it is not straightforward to find the differences in the densities of the two amorphous forms.

It would have been very useful to compare the structure factors of a-V_2O_5 obtained using these two methods, but unfortunately high-quality x-ray diffraction has not been reported either on vapor-deposited amorphous or on splat-cooled glassy forms. It should be pointed out that the structure of splat-cooled V_2O_5 had been previously interpreted to have coexisting fourfold- and fivefold-coordinated vanadium atoms.[12] On the other hand, based on the present Raman spectra, one can say with certainty that the local structure and coordination in a-V_2O_5 is similar to that of the α phase and not the β phase. This is because the characteristic Raman peaks of the β phase are not present in the recovered V_2O_5. It should also be pointed out that nonhydrostatic conditions were used in the present study, as this is known to advance the amorphization pressure. Use of suitable quasihydrostatic pressure-transmitting media, know to remain hydrostatic only up to certain pressures, is likely to postpone the amorphization to a higher pressure. The present results should motivate other researchers to take up such studies.

IV. SUMMARY AND CONCLUSIONS

To summarize, we have reported on a high-pressure amorphous form of V_2O_5 above 40 GPa under nonhydrostatic conditions. The evolution to an amorphous state is preceded by the growth of disorder in the high-pressure β phase, as concluded from the broadening and weakening of the x-ray diffraction patterns. Similar consequences of the disorder are found in the Raman spectra. Although the sample remains amorphous upon the release of pressure, the high-pressure amorphous state is not quenchable to the ambient, pointing to the possibility of polyamorphism in this system. Raman spectra show evidence of only doubly coordinated oxygen in the high-pressure amorphous form, while the recovered amorphous form has V=O bonds. A comparison of the Raman spectra of the recovered and the vapor-deposited a-V_2O_5 forms suggests that although both of these have disordered arrangements of VO_5-like structural units, the intermediate-range orders are not identical.

ACKNOWLEDGMENTS

A.K.A. thanks The University of Tokyo for the Visiting Professor position, Dr. C. S. Sundar for interest in the work, and the Director of IGCAR for support.

*Author to whom all correspondence should be addressed: aka@igcar.gov.in

[1]K. Samwer, H. J. Fecht, and W. L. Johnson, in *Glassy Metals III*, edited by H. Beck and H. J. Guntherodt (Springer, Berlin, 1994), p. 5.
[2]R. Singh and J. S. Chakravarthi, Phys. Rev. B **55**, 5550 (1997).
[3]A. Dalvi and K. Shahi, J. Non-Cryst. Solids **341**, 124 (2004).
[4]S. Chakraborty, K. Suzuki, and H. Sakata, Mater. Lett. **34**, 341 (1998).
[5]A. K. Arora, Solid State Commun. **115**, 665 (2000).
[6]A. K. Arora, V. S. Sastry, P. C. Sahu, and T. A. Mary, J. Phys.: Condens. Matter **16**, 1025 (2004).
[7]A. K. Arora, R. Nithya, T. Yagi, N. Miyajima, and T. A. Mary, Solid State Commun. **129**, 9 (2004).
[8]R. J. Hemley, L. C. Chen, and H. K. Mao, Nature (London) **338**, 638 (1989).
[9]G. D. Mukherjee, S. N. Vaidya, and V. Sugandhi, Phys. Rev. Lett. **87**, 195501 (2001).
[10]O. Mishima, L. D. Calvert, and E. Whalley, Nature (London) **314**, 76 (1985).
[11]S. K. Deb, M. Wilding, M. Somayazulu, and P. F. McMillan, Nature (London) **414**, 528 (2001).
[12]M. Nabavi, C. Sanchez, and J. Livage, Philos. Mag. B **63**, 941 (1991).
[13]S. H. Lee, H. M. Cheong, M. J. Seong, P. Liu, C. E. Tracy, A. Mascarenhas, J. R. Pitts, and S. K. Deb, Solid State Ion. **165**, 111 (2003).
[14]R. Remirez, B. Casal, L. Utrera, and E. R. Hitzky, J. Phys. Chem. **94**, 8965 (1990).
[15]C. R. Aita, Y.-L. Liu, M. L. Kao, and S. D. Hansen, J. Appl. Phys. **60**, 749 (1986).
[16]H. Hirashima, M. Ide, and T. Yoshida, J. Non-Cryst. Solids **86**, 327 (1986).
[17]M. E. A. Dompablo, J. M. G. Amores, U. Amador, and E. Morán, Electrochem. Commun. **9**, 1305 (2007).
[18]A. B. Cheremisin, S. V. Loginova, A. A. Velichko, V. V. Putrolaynen, A. L. Pergament, and A. M. Grishin, J. Phys.: Conf. Series **100**, 052096 (2008).
[19]A. Gies, B. Pecquenard, A. Benayad, H. Martinez, D. Gonbeau, H. Fuess, and A. Levasseur, Solid State Ion. **176**, 1627 (2005).
[20]T. Gallasch, T. Stockhoff, D. Baither, and G. Schmitz, J. Power Source **196**, 428 (2011).
[21]N. Fateh, G. A. Fontalvo, and C. Mitterer, J. Phys. D **40**, 7716 (2007).
[22]S. Dhawan, A. G. Vedeshwar, and R. P. Tandon, J. Phys. D **44**, 215404 (2011).
[23]K. Kusaba, E. Ohshima, Y. Syono, and T. Kikegawa, J. Cryst. Growth **229**, 467 (2001).
[24]I. Loa, A. Grzechnik, U. Schwarz, K. Syassen, M. Hanfland, and R. K. Kremer, J. Alloys Compd. **317–318**, 103 (2001).
[25]J. M. G. Amores, N. Biskup, U. Amador, K. Persson, G. Ceder, E. Moran, and M. E. A. Dompablo, Chem. Mater. **19**, 5262 (2007).
[26]T. Suzuki, S. Saito, and W. Arakawa, J. Non-Cryst. Solids **24**, 355 (1977).
[27]A. Grzechnik, Chem. Mater. **10**, 2505 (1998).
[28]V. P. Filonenko, M. Sundberg, P.-E. Werner, and I. P. Zibrov, Acta Crystallogr. B **60**, 375 (2004).
[29]P. Balog, D. Orosel, Z. Cancarevic, C. Schon, and M. Jansen, J. Alloys Compd. **429**, 87 (2007).
[30]O. L. Anderson, D. G. Isaak, and S. J. Yamamoto, J. Appl. Phys. **65**, 1534 (1989).
[31]T. R. Ravindran and J. V. Badding, Solid State Commun. **121**, 391 (2002).
[32]D. Machon, A. Grzechnik, and K. Friese, J. Phys.: Condens. Matter **21**, 405405 (2009).
[33]J. S. Tse, D. D. Klug, S. Desgreniers, J. S. Smith, and R. Dutrisac, Europhys. Lett. **86**, 56001 (2009).
[34]B. K. Godwal, S. Speziale, S. M. Clark, J. Yan, and R. Jeanloz, J. Phys. Chem. Solids **71**, 1059 (2010).
[35]Z. Jenei, H. Liermann, H. Cynn, J.-H. Klepeis, B. Baer, and W. Evans, Phys. Rev. B **83**, 054101 (2011).
[36]T. R. Ravindran, A. K. Arora, and T. A. Mary, Phys. Rev. Lett. **84**, 3879 (2000).
[37]A. K. Arora, T. Okada, and T. Yagi, Phys. Rev. B **81**, 134103 (2010).
[38]D. Daisenberger, M. Wilson, P. F. McMillan, R. Q. Cabrera, M. C. Wilding, and D. Machon, Phys. Rev. B **75**, 224118 (2007).
[39]A. C. Geiculescu and H. J. Rack, J. Sol-Gel Sci. Technol. **20**, 13 (2001).
[40]R. P. Ozero, Usp. Khim. **24**, 951 (1955).
[41]R. J. H. Clark, *The Chemistry of Titanium and Vanadium* (Elsevier, New York, 1968).
[42]C. Julien, G. A. Nazri, and O. Bergstrom, Phys. Status Solidi B **201**, 319 (1997).
[43]L. Abello, E. Husson, Y. Repelin, and G. Lucazeau, Spectrochim. Acta A **39**, 641 (1983).
[44]J. M. Jehng, F. D. Hardcastle, and I. E. Wachs, Solid State Ion. **32–33**, 904 (1989).
[45]V. V. Brazhkin and A. G. Lyapin, J. Phys.: Condens. Matter **15**, 6059 (2003).
[46]S. Aasland and P. F. McMillan, Nature (London) **369**, 633 (1994).
[47]P. H. Poole, T. Grande, C. A. Angell, and P. F. McMillan, Science **275**, 322 (1997).
[48]S. Sampath, C. J. Benmore, K. M. Lantzky, J. Neuefeind, K. Leinenweber, D. L. Price, and J. L. Yarger, Phys. Rev. Lett. **90**, 115502 (2003).
[49]A. K. Arora, T. Sato, and T. Yagi, J. Phys.: Condens. Matter **23**, 112207 (2011).